Biotechnol Lett (2013) 35:657–661
DOI 10.1007/s10529-012-1121-2

ORIGINAL RESEARCH PAPER

Hydroxyapatite/regenerated silk fibroin scaffold-enhanced osteoinductivity and osteoconductivity of bone marrow-derived mesenchymal stromal cells

Jia Jiang · Wei Hao · Yuzhuo Li · Jinrong Yao · Zhengzhong Shao · Hong Li · Jianjun Yang · Shiyi Chen

Received: 7 October 2012 / Accepted: 7 December 2012 / Published online: 18 December 2012

Abstract A novel hydroxyapatite/regenerated silk fibroin scaffold was prepared and investigated for its potential to enhance both osteoinductivity and osteoconductivity of bone marrow-derived mesenchymal stromal cells in vitro. Approx. 12.4 ± 0.06 % (w/w) hydroxyapatite was deposited onto the scaffold, and cell viability and DNA content were significantly increased (18.5 ± 0.6 and 33 ± 1.2 %, respectively) compared with the hydroxyapatite scaffold after 14 days. Furthermore, alkaline phosphatase activity in the novel scaffold increased 41 ± 2.5 % after 14 days compared with the hydroxyapatite scaffold. The data indicate that this novel hydroxyapatite/regenerated silk fibroin scaffold has a positive effect on osteoinductivity and osteoconductivity, and may be useful for bone tissue engineering.

Keywords Bone tissue engineering · Hydroxyapatite · Osteoconductivity · Osteoinductivity · Regenerated silk fibroin

J. Jiang · Y. Li · H. Li · J. Yang · S. Chen (✉)
Fudan University Sports Medicine Center, Department of Sports Medicine and Arthroscopy Surgery, Huashan Hospital, Fudan University, No. 12 Wulumuqi Zhong Road, Shanghai 200040, China
e-mail: biochenjun@sjtu.edu.cn

W. Hao · J. Yao · Z. Shao
Laboratory of Advanced Materials, National Key Laboratory of Molecular Engineering of Polymers, Department of Macromolecular Science, Fudan University, Shanghai 200433, China

Introduction

As a fibrous protein, silk fiber from *Bombyx mori* has been used as biomedical material due to its unique porous structure, biocompatibility, permeability, biodegradability, and minimal inflammatory reaction (Altman et al. 2003; Jin et al. 2004). However, it still has problematic characteristics for further clinical applications and use in industrial processes, such as its low stiffness and high production cost (Freed et al. 1994; Zhou et al. 2009). For this reason, several attempts have been made to improve the properties of silk biomaterials, and this field has become a rapidly growing area of tissue engineering research. Research has demonstrated that the main inorganic component of human bone tissues, hydroxyapatite (HA), enhances the compressive strength of silk biomaterials and also induces new bone formation (Na et al. 2007). Therefore, the HA/silk scaffold is an attractive candidate for bone tissue engineering and has thus been widely studied in the last decade (Kim et al. 2008; Bhumiratana et al. 2011).

Recently, we developed a novel method to convert silk fiber into regenerated silk fibroin (RSF) solutions that can be subsequently reconstituted into macroporous architecture (Cao et al. 2007). Research has demonstrated that RSF is stronger, tougher, and more extensible than natural silk fiber (Chen et al. 2009; Zhou et al. 2011).

Here, we combined the advantages of both RSF and HA to prepare a novel HA/RSF scaffold. After first characterizing the scaffold it was then investigated for its potential in osteoregenerative applications. Both

HA/RSF scaffold osteoconductivity and osteoinductivity were assessed by culturing rat bone marrow-derived mesenchymal stromal cells (BMSCs) on the scaffold surface and observing cell morphology, cell viability, DNA content, gene expression, alkaline phosphatase (ALP) activity, etc.

Materials and methods

Preparation of the RSF scaffold

The RSF scaffold was prepared according to previous methods (Cao et al. 2007). Briefly, *B. mori* silk was degummed in 0.5 % (w/v) Na_2CO_3 at 95 °C for 1 h, washed with copious distilled water, and then dried. The degummed silk was dissolved in 9.5 mM LiBr. After filtration, the fibroin solution was dialyzed against deionized water for four days at room temperature with a 12 kDa cut-off, semi-permeable membrane for salt removal. The dialyzed silk fibroin solution was centrifuged at $\sim 5{,}000 \times g$ for 10 min. Next, 10 % (w/w) ethanol was added to the RSF solution under gentle stirring at 25 °C over 2 min, and then held at −80 °C for 24 h. The sample was defrosted by freeze-drying. Dry particles of RSF were obtained by lyophilization with a freezing dryer after stable RSF microspheres were collected by centrifugation at $\sim 10{,}000 \times g$ for 30 min.

HA/RSF scaffold preparation

HA was deposited onto the RSF scaffold using an alternate soaking process (Wang et al. 2007). In brief, the RSF scaffold was immersed in 200 mM $CaCl_2$ in a Petri dish and shaken at 150 rpm for 1 h at 37 °C. The scaffold was then blotted onto filter paper to remove excess water and then immersed in 120 mM Na_2HPO_4 for 1 h. After soaking alternately for three cycles, HA/RSF scaffolds were washed in distilled water and air-dried at room temperature for 24 h. The morphology of the RSF and HA/RSF scaffolds was observed using scanning electron microscopy (SEM).

Scaffold weight change after HA coating

The dry weights of the RSF and HA/RSF scaffolds were measured and the weight percentage of HA deposited onto the silk scaffolds was calculated as:

$$\text{Percentage deposition of HA (w/w, \%)} = (W_t - W_r)/W_t \times 100\,\%,$$

where W_r is weight of RSF scaffold, W_t is weight of HA/RSF scaffold.

Cell isolation, seeding, and culturing onto scaffolds

BMSCs were isolated from five New Zealand white rabbits (average weight, 2.5 kg) according to procedures described previously (Shao et al. 2006), and cultured in Dulbecco's modified Eagle's medium at 37 °C with 5 % CO_2. Scaffolds were sterilized by autoclaving and seeded with BMSCs at 1.5×10^5 cells per scaffold.

MTT assay

The MTT assay was carried out as previously described (Wang et al. 2007). Briefly, culture medium was removed and 100 µl MTT was added to each well. After incubation for 4 h, the medium was discarded and the precipitated formazan was dissolved in dimethyl sulfoxide. The A_{570} was then measured in a microplate reader.

DNA content analysis

The RSF and HA/RSF scaffolds from various time intervals were washed in phosphate-buffered saline and lysed in 0.2 % (w/v) Triton X-100 and 5 mM $MgCl_2$. A Pico Green assay was used to measure the total amount of DNA.

ALP activity assessment

The ALP activity of cells cultured on RSF and HA/RSF scaffolds was detected at several time intervals using a phosphatase substrate kit. ALP activity was expressed as *p*-nitrophenol produced in nmol/min/mg protein.

Gene expression analysis by quantitative real-time PCR (RT-PCR)

Gene expression of various proteins involved in osteogenesis, including Runt-related transcription factor 2 (Runx2), collagen type I, osteopontin (OPN), and osteonectin (ON) were analyzed in BMSCs seeded

with RSF and HA/RSF scaffolds. Primer sequences of the genes were obtained from published literature Fiedler et al. (2002). Total RNA was extracted from each cell sample using TRIzol and the cDNA was synthesized from total RNA. Quantitative PCR (QPCR) was carried out using SyberGreen I in a Rotor-Gene 3000. To correct for differences in RNA quality and quantity among samples, the data were normalized to that of GAPDH.

Statistical analysis

Results are expressed as the mean ± SD. Multiple comparisons involved single factor analysis of variance (ANOVA) using SPSS Statistics 17.0 statistical software package. P values <0.05 were considered statistically significant.

Results and discussion

HA/RSF scaffold morphology

SEM images revealed a porous, spongy morphology of the HA/RSF scaffold, while HA nanoparticles were deposited uniformly on the surface of the silk sponge without any apparent effect on scaffold pore architecture (Fig. 1a). As shown in Fig. 1b, high-magnification SEM images confirmed the presence of dense flake-like HA crystals emanating from the surface and throughout the pore walls of the silk framework. Approx. 12.4 ± 0.06 % (w/w) of HA was deposited on the silk scaffold after HA deposition by weight quantification analysis. Energy dispersive X-ray (EDX) analysis (Fig. 1c) revealed that the ratio of Ca and P was 1.52, similar to the composite of mature bone.

SEM images of BMSC-seeded scaffolds after 1 day in culture revealed that HA/RSF scaffolds support the adhesion and proliferation of BMSCs (Fig. 1d). After 7 days, BMSCs adhered to the surface of the HA/RSF scaffold and exhibited a spreading-out phenotype (Fig. 1e). After 14 days, it was obvious that typical osteoblast-like cells appeared in the scaffolds (Fig. 1f).

Cell viability and proliferation

As shown in Fig. 2, after 14 days the cell viability and DNA content of BMSCs increased significantly (18.5 ± 0.6 and 33.2 ± 1.2 %, respectively) on the

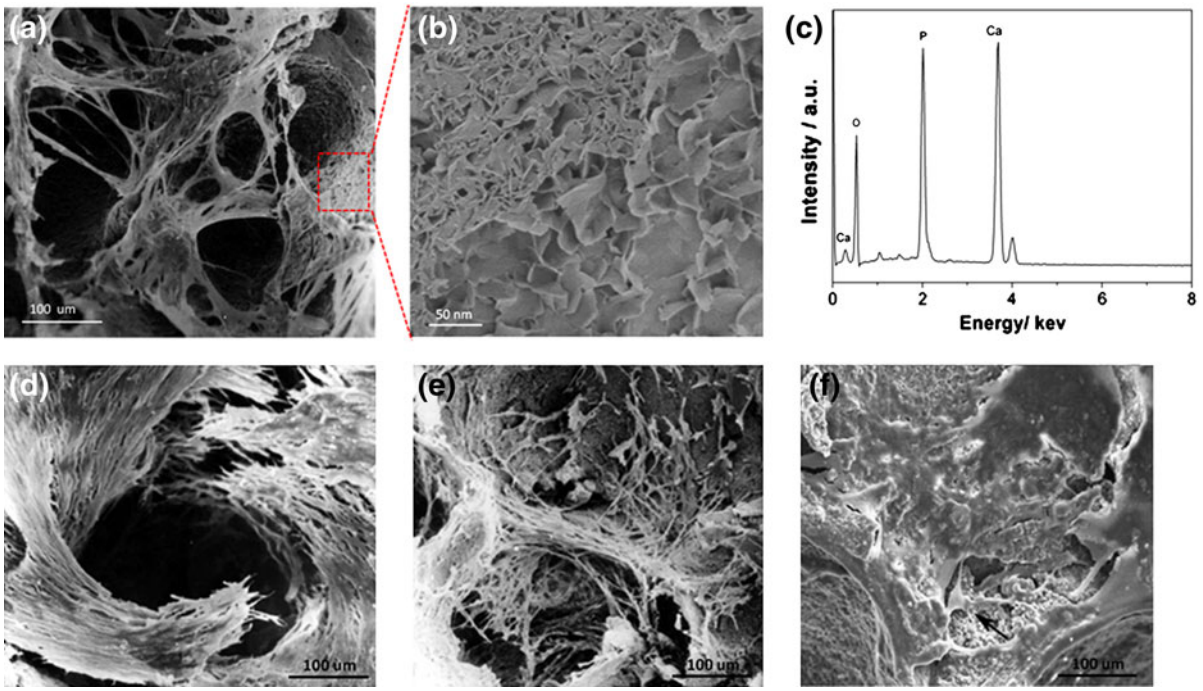

Fig. 1 (**a**) SEM image and (**b**) high-magnification SEM image of a prepared HA/RSF scaffold. (**d**) Energy dispersive X-ray (EDX) analysis of a prepared HA/RSF scaffold. SEM images of BMSCs seeded onto a HA/RSF scaffold after (**c**) 1 day, (**e**) 7 days, and (**f**) 14 days. The *blank arrow* in (**f**) indicates typical osteoblast-like cells

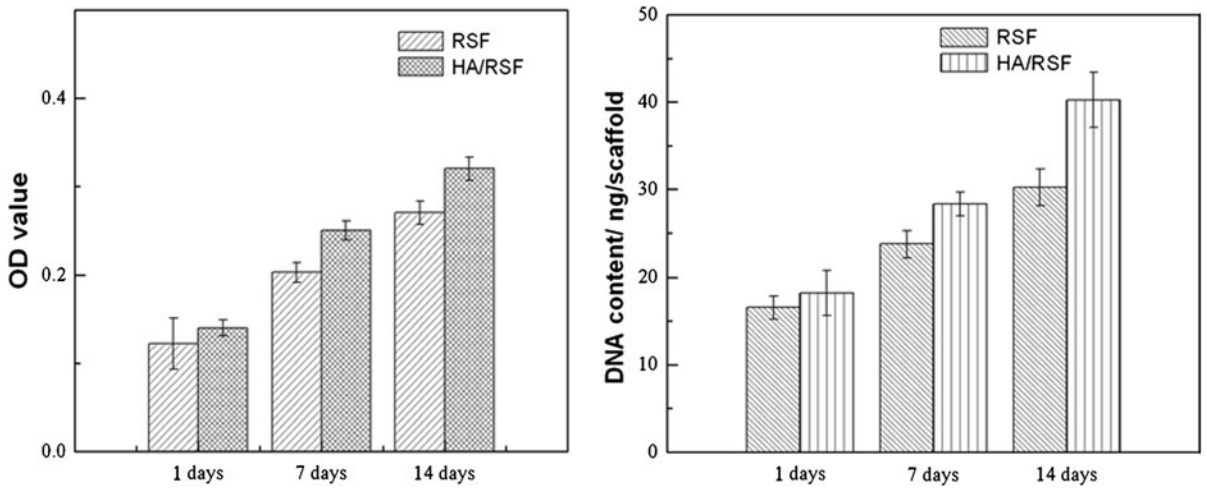

Fig. 2 (**a**) MTT assay and (**b**) DNA content analysis of BMSCs seeded onto a HA/RSF scaffold at different time intervals. Results are shown as the mean ± SD ($n = 5$)

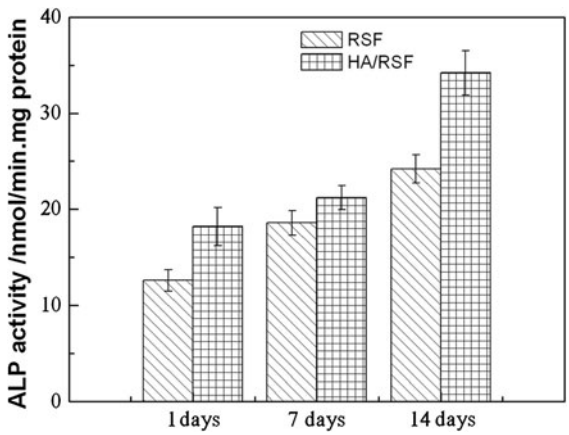

Fig. 3 Detection of ALP activity for RSF and HA/RSF scaffolds at different time intervals. Results are shown as the mean ± SD ($n = 5$)

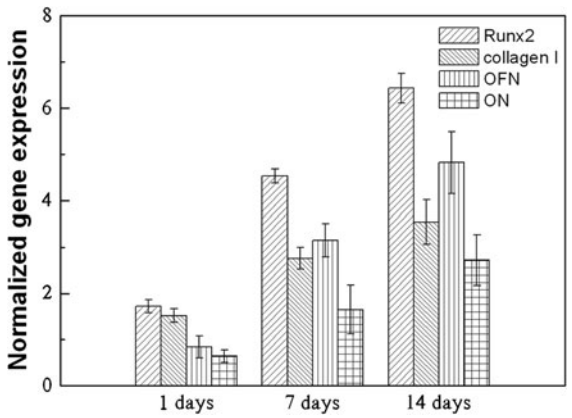

Fig. 4 Gene expression analysis of BMSCs seeded onto both RSF and HA/RSF scaffolds at different time intervals by quantitative RT-PCR. Results are shown as the mean ± SD ($n = 5$)

HA/RSF scaffold compared to the HA scaffold. Both the MTT assay and DNA content analysis suggested that BMSCs seeded on the HA/RSF scaffold increased and remained viable over 2 weeks in culture, indicating that the scaffold supported the proliferation of BMSCs.

ALP activity and gene expression analysis by quantitative RT-PCR

ALP has been implicated as a marker of osteogenic differentiation that is expressed early in the differentiation process. As shown in Fig. 3, ALP activity increased by 41.3 ± 2.5 % after 14 days in HA/RSF scaffolds compared with that in RSF scaffolds. Furthermore, as shown in Fig. 4, after 2 weeks in culture, gene expression analysis of bone-related genes, such as Runx2, collagen type I, OPN, and ON, were upregulated in the BMSC-seeded HA/RSF scaffolds compared with BMSC-seeded RSF scaffolds. These observations suggest that prepared HA/RSF scaffolds may enhance the differentiation of BMSCs toward osteoblast cells.

Conclusions

We successfully fabricated HA/RSF hybrid scaffolds that combine the advantages of both RSF and HA. The feasibility of these HA/RSF hybrid scaffolds as implants for bone damage was evaluated in vitro. Our results suggest that the incorporation of HA not only increases the surface roughness of scaffolds, but also enhances the viability and proliferation of BMSCs on the scaffold surface. Furthermore, these scaffolds improve the differentiation of BMSCs toward osteoblast cells in vitro. In conclusion, our work demonstrates that HA/RSF scaffolds may be a promising biomaterial for bone tissue engineering in the future.

Acknowledgments This work was supported by the Grants from the Young Project of National Natural Science Foundation of China (81000816), 973 Project from the Ministry of Science and Technology of China (No. 2009CB930000), and the Project of Shanghai Municipal Science and Technology Commission (11JC1401700 and 12ZR1415800).

References

Altman GH, Diaz F, Jakuba C, Calabro T, Horan RL, Chen J, Lu H, Richmond J, Kaplan DL (2003) Silk-based biomaterials. Biomaterials 24(3):401–416

Bhumiratana S, Grayson WL, Castaneda A, Rockwood DN, Gil ES, Kaplan DL, Vunjak-Novakovic G (2011) Nucleation and growth of mineralized bone matrix on silk-hydroxyapatite composite scaffolds. Biomaterials 32(11):2812–2820

Cao Z, Chen X, Yao J, Huang L, Shao Z (2007) The preparation of regenerated silk fibroin microspheres. Soft Matter 3(7):910–915

Chen X, Knight DP, Shao Z (2009) [Small beta]-turn formation during the conformation transition in silk fibroin. Soft Matter 5(14):2777–2781

Fiedler J, Röderer G, Günther K-P, Brenner RE (2002) BMP-2, BMP-4, and PDGF-bb stimulate chemotactic migration of primary human mesenchymal progenitor cells. J Cell Biochem 87(3):305–312

Freed LE, Vunjak-Novakovic G, Biron RJ, Eagles DB, Lesnoy DC, Barlow SK, Langer R (1994) Biodegradable Polymer Scaffolds for Tissue Engineering. Nat Biotech 12(7):689–693

Jin H-J, Chen J, Karageorgiou V, Altman GH, Kaplan DL (2004) Human bone marrow stromal cell responses on electrospun silk fibroin mats. Biomaterials 25(6):1039–1047

Kim HJ, Kim U-J, Kim HS, Li C, Wada M, Leisk GG, Kaplan DL (2008) Bone tissue engineering with premineralized silk scaffolds. Bone 42(6):1226–1234

Na K, Sw Kim, Sun BK, Woo DG, Yang HN, Chung HM, Park KH (2007) Osteogenic differentiation of rabbit mesenchymal stem cells in thermo-reversible hydrogel constructs containing hydroxyapatite and bone morphogenic protein-2 (BMP-2). Biomaterials 28(16):2631–2637

Shao XX, Hutmacher DW, Ho ST, Goh JCH, Lee EH (2006) Evaluation of a hybrid scaffold/cell construct in repair of high-load-bearing osteochondral defects in rabbits. Biomaterials 27(7):1071–1080

Wang H, Li Y, Zuo Y, Li J, Ma S, Cheng L (2007) Biocompatibility and osteogenesis of biomimetic nano-hydroxyapatite/polyamide composite scaffolds for bone tissue engineering. Biomaterials 28(22):3338–3348

Zhou G, Shao Z, Knight DP, Yan J, Chen X (2009) Silk fibers extruded artificially from aqueous solutions of regenerated *Bombyx mori* silk fibroin are tougher than their natural counterparts. Adv Mater 21(3):366–370

Zhou J, Fang T, Wen J, Shao Z, Dong J (2011) Silk coating on poly(e-caprolactone) microspheres for the delayed release of vancomycin. J Microencapsul 28(2):99–107